2018-06-01

An Introductory Study of Solid Materials for Capture and Catalysis of Waste Stream Chemicals

Steven Kyle Butler
Brigham Young University

An Introductory Study of Solid Materials for Capture and Catalysis of Waste Stream Chemicals

Steven Kyle Butler

A thesis submitted to the faculty of
Brigham Young University
in partial fulfillment of the requirements for the degree of

Master of Science

Kara Stowers, Chair
David J. Michaelis
Richard K. Watt

Department of Chemistry and Biochemistry

Brigham Young University

ABSTRACT

An Introductory Study of Solid Materials for Capture and
Catalysis of Waste Stream Chemicals

Steven Kyle Butler
Department of Chemistry and Biochemistry, BYU
Master of Science

Heterogeneous catalysts are key materials in research and industry. Herein we study two materials in different stages of development toward being applied as heterogeneous catalysts. First, MoO_3SnO_2 was synthesized and studied as a catalytic system similar to Sn-beta zeolites. While the Mo-based catalyst did not show similar activity to Sn-beta, it did show interesting reactivity in activating carbonyls and oxidizing organic substrates. Second, a method was developed for grafting amines onto carboxylic acid functionalized carbon nanotubes for CO_2 capture. The method was successful for grafting monomer ethylamine groups onto CNT and can be further developed to allow for polymeric amine groups to be grafted.

Keywords: molybdenum, tin, carbon nanotubes, heterogeneous, catalysis, green chemistry, organic, inorganic

ACKNOWLEDGEMENTS

Many thanks need to be given to my wife and editor Starla Butler for her help and support throughout my research and writing. To my undergraduate research assistants who helped along the way, Spencer Lee and Isaac Cloward. Also, all the professors and mentors along the way, especially Dr. Stowers for guiding and teaching me these 2 years.

TABLE OF CONTENTS

LIST OF TABLES

LIST OF FIGURES

1 Solid materials for capture and coupling of small organic molecules

This work is focused on the use of waste stream chemicals as building blocks for useful products. This was studied using a solid catalyst in the presence of either a liquid or gaseous reactant phase. The liquid phase reactions were carried out in batch reactors and the gas phase reactions were carried out in a flow reactor. The use of a catalyst that is a different phase from the reactants is known as heterogeneous catalysis. Heterogeneous catalysis has several benefits over traditional homogeneous catalysis. Heterogeneous catalysts are generally easier to remove from products than homogeneous catalysts (providing that the products are not solid). Heterogeneous catalysts usually have a higher reusability as they can often be removed from the reaction and re-activated for further use.

While there are many benefits to heterogeneous catalysts there are also some downsides. Characterization of heterogeneous catalysts is often labor intensive—as they are almost exclusively solids, they cannot be analyzed by traditional NMR techniques. Powder X-ray Crystallography (P-XRD) is generally used to characterize the elements present in a catalyst, along with X-ray Photoelectron Spectroscopy (XPS) to characterize the elemental oxidation states present and surface composition. Surface area is determined by the Brunauer-Emmett-Teller technique (BET) as well as chemical vapor desorption experiment to determine the acidity and basicity of the metal sites. While characterization can be difficult, the rewards of

understanding the composition and active sites of heterogeneous catalysis give important insight into the chemistry that is occurring. This understanding can be used to increase the activity and selectivity of these catalysts.

One part of this work involved synthesis of a carbon nanotube (CNT) and polyethylenimine (PEI) material to capture CO_2. The material later will be used as a scaffold for catalysts that can react with the captured CO_2. While not yet a heterogeneous catalyst, it is a key beginning step in making a heterogeneous catalytic system.

The other part is the synthesis, characterization, and catalytic testing of MoO_3SnO_2. This catalyst has recently shown interesting reactivity, in the oxidation of dimethylether to formaldehyde.[1] The catalyst was synthesized, characterized, and tested in a wide variety of reactions to determine its catalytic similarity to Sn-beta zeolites, another Lewis acidic catalyst.

Both parts of this work have involved synthesis of solid materials—one a heterogeneous Mo-based catalyst and the other a carbon nanotube based support decorated with amines. While the materials made were very different, the techniques used to characterize them were similar. For both projects the surface of the material was important. The CNT surface was characterized using Brunauer-Emmett-Teller technique (BET) and followed up with a Barrett-Joyner-Halenda (BJH) analysis of the physical properties of the pores. The MoO_3SnO_2 surface was characterized using powder X-ray crystallography. Insight into the bonding environments of both materials were observed using spectroscopy: MoO_3SnO_2 by Raman spectroscopy and The CNTs by UV-Vis spectroscopy.

2 Molybdenum Tin Mixed Metal Oxides as a Catalyst for Oxidation and Coupling Reactions

2.1 Introduction

Molybdenum is an earth abundant and relatively eco-friendly element, unlike most of the transition metals which are either toxic or rare. One of the purposes of this project was to expand the use of molybdenum-based catalysts. Specifically, I aimed to explore the possibility of MoO_3SnO_2 catalyzing reactions in a similar way as Sn-beta zeolite catalysts.

The main purpose of this project was to synthesize a previously reported MoO_3SnO_2 heterogeneous catalyst and characterize the catalyst through the materials characterization techniques used in our lab.[1] The catalyst was then tested against a wide range of reactions previously reported as catalyzed by Sn-beta zeolites. The results of these reactions would provide evidence for the central hypothesis that MoO_3SnO_2 exhibits similar but distinct reactivity to Sn-beta zeolites as both are good Lewis-acidic catalysts.

2.2 Sn-Beta Zeolites

Beta zeolites are ordered arrays of Si, Al, and O. They form a large network similar to that shown in Figure 1. These zeolite structures can be doped with metals to affect their

properties. Sn-beta zeolites are generally prepared by treating beta zeolite with $SnCl_4$ and give the structure shown in Figure 1.[2]

Figure 1: Sn-Beta Zeolite[3]

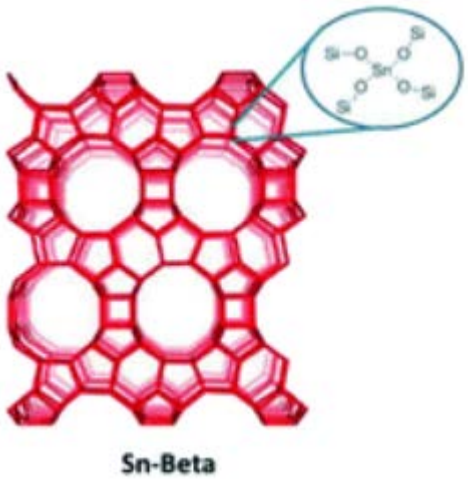

Silicate based zeolites doped with transition metals have been used as both solid Lewis acidic and solid Lewis basic catalysts.[4] Common uses of Sn doped zeolites have been the Baeyer-Villiger oxidation of small molecules, conversion of small ketones into esters,[5] and isomerization of molecules such as glucose.[6] The substrates are limited to small molecules because the substrates must diffuse into the small pores of the zeolite.

This catalytic activity comes from the acidic properties of the Sn^{4+}. Tin(IV) is a good Lewis acid as it is electron deficient and so can be used in a wide variety of Lewis acid catalyzed reactions. Our hypothesis was that the cooperation of Mo and Sn would create a similar Lewis acid system with unique reactivity and selectivity using readily available oxide components and

without a highly engineered structure; the pore sizes would also allow a larger subset of molecules to react.

2.3 Molybdenum Trioxide

MoO_3 is an earth abundant compound (more abundant in ground water than Fe due to solubility[7,8]) with relatively low toxic effects. These properties have helped Mo research be fueled by current green chemistry pushes. It has been used for a wide variety of reactions including hydrodeoxygenation[9] and NO_x reduction.[10] The MoO_3 includes a Lewis acidic Mo center that can undergo IV-VI oxidation cycles and oxidize organic molecules readily. As previously stated we sought to harness this Lewis acidity to catalyze reactions.

2.4 Molybdenum-Tin

Zhang et. al reported on a molybdenum tin mixed oxide catalyst that showed activity for the formation of methyl formate and formaldehyde using dimethyl ether as a substrate.[1] The mechanism of the reaction occurred through decomposition of the dimethyl ether to a surface bound methoxy group (the fate of the CH_3^+ was not reported). The methoxy group is then oxidized to formaldehyde. This mechanism is shown in Figure 2.

Figure 2: MoO_3SnO_2 Mechanism[1]

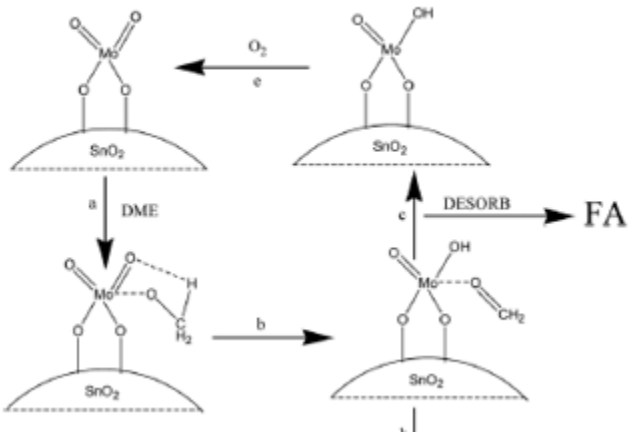

However, there are some issues with the reported mechanism. How the C-O bond is broken and where the CH_3 fragment goes are unclear. The O-CH_3 is deprotonated but it is not shown where the electrons migrate to. Our more likely mechanism shows the Mo coordinating the dimethyl ether through an agnostic coordination to the C-O bond then the oxidative addition of the C-O onto the Mo is followed by the CH_3 deprotonation of the Mo-OH as shown in Figure 3. In both mechanisms molybdenum shows the ability to break both C-O bonds and C-H bonds.

Figure 3: MoO_3SnO_2 Dimethylether Catalytic Cycle

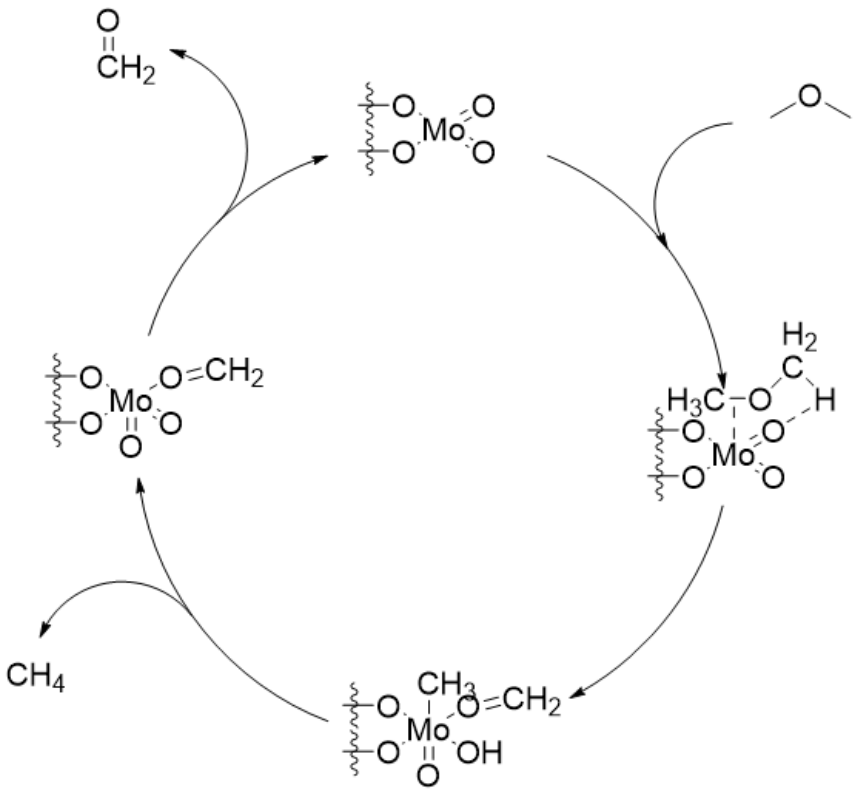

The above oxidation of alcohol and aldehydes to esters is similar to recent Sn-beta zeolite catalysts. We attempted to replicate other relevant Sn-beta zeolite catalyzed reactions with the simpler molybdenum tin oxide, with the hypothesis that the combination of Sn and Mo sites would facilitate unique changes to reactivity and selectivity by the Sn-O-Mo bond increasing the Lewis acidity of the Mo and making it a comparable Lewis acid catalyst to others that have been reported. The MoO_3 on the surface of the SnO_2 should mean the substrates are not limited by what can diffuse into the pores as with the zeolites.

2.5 Catalyst Synthesis

MoO_3SnO_2, with a Mo:Sn ratio of 1:2, was synthesized by a co-precipitation method. In a typical synthesis, 1.74 grams of AHM ($(NH_4)_6Mo_7O_{24}\cdot 4H_2O$) was dissolved in 20 mL of water. 5.13 grams of sodium stannate was dissolved in 50 mL of water. The two solutions were mixed while stirring vigorously. The solution was heated to 60 °C while stirring and 3.7 mL of concentrated nitric acid was added. The solution was kept at 60 °C for 2 hours then allowed to cool to room temperature. The solution was then filtered and rinsed with water before being dried at 90 °C overnight. The solid was then calcined at 800 °C for 8 hours with a ramp rate of 13 °C/min. After calcination the catalyst was ground until a visually homogenous fine powder was formed.

The original preparation method was adapted from Zheng et. al.[1] Further modifications were adapted from a later paper from the same group.[11] While attempting to synthesize this catalyst we found the methods sections rather vague. No papers reported the concentration of the AHM and tin (either $SnCl_x$ or sodium stannate) solutions. Our experiments showed that the concentration of the solutions must be close to saturation to get a proper co-precipitation of the desired product. Dilute solutions did not produce a significant amount of precipitate of the desired catalyst.

2.6 Catalyst Characterization

A couple of techniques were used to characterize the catalyst. Powder x-ray diffraction (P-XRD) was used to determine the structure of the MoO_3 and SnO_2. Similarly, Raman spectroscopy was used to characterize the nature of the MoO_3 clusters and isolated domains.

2.6.1 P-XRD

Powder x-ray diffraction crystallography was used to characterize the morphology of the catalyst. We characterized the samples with an X'Pert Pro, PANalytical with a Cu/Ka radiation source (40 kV, 40 mA). The P-XRD spectrum is shown in Figure 4 and shows very small peaks, some barely above the noise, that correspond to MoO_3 (23.5, 26.5, 28.5). According to Il'in et al. the disperse MoO_3 domains are shown by the lack of peaks in the P-XRD spectrum.[12] Sharp peaks are characteristic of more crystalline samples; since there are small sharp peaks, most of the particles are most likely smaller than the 2-nm limit of the instrument and thus very dispersed on the SnO_2 surface. The SnO_2 peaks tend to be very broad and hard to identify, especially with low signal.

Figure 4: P-XRD Spectrum of MoO_3SnO_2

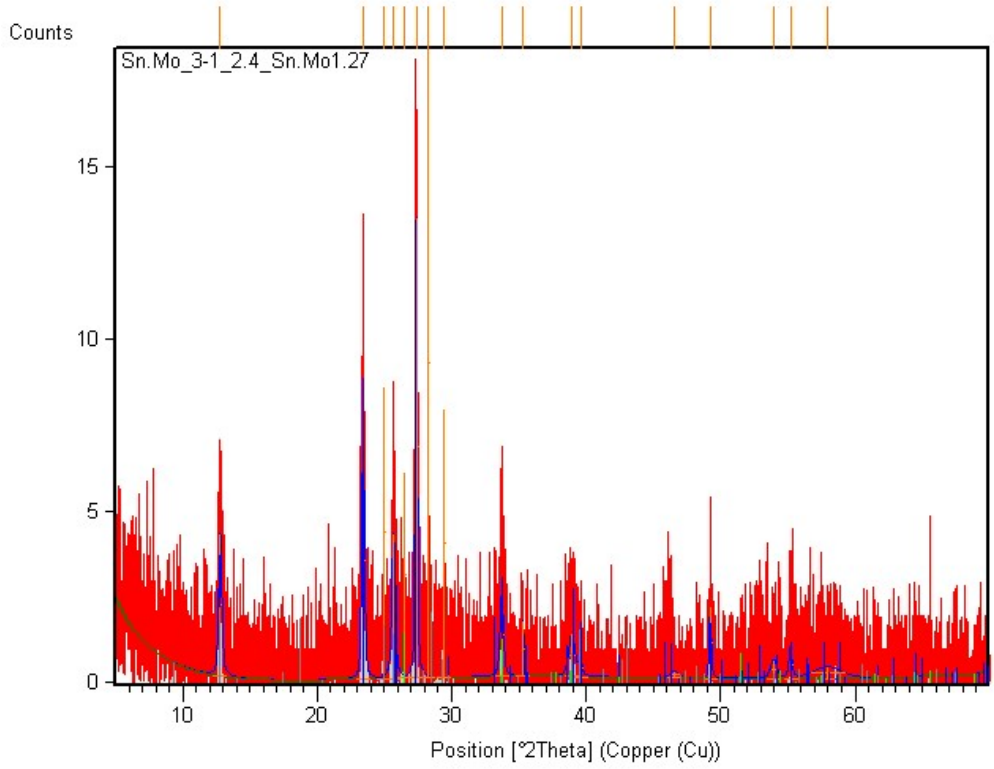

2.6.2 Raman Spectroscopy

The functional groups were identified with Raman spectroscopy. We used a Renishaw inVia Raman Microscope spectrometer with a 785-nm wavelength laser (1% power) with a 5s exposure time and a spectral range of 45.87 to 1273.62 cm^{-1}. Liu et al. identified the disperse MoO_3 domains by their Raman spectra shown in Figures 5 and 6.[13] They assigned bands at the following: 636 cm^{-1}, 777 cm^{-1} are attributed to SnO_2 crystallites. 864-870 cm^{-1}, Mo-O-Mo bridge. 953-967 cm^{-1}, Terminal Mo=O. 672 cm^{-1}, 825 cm^{-1}, 1001 cm^{-1}, crystalline MoO_3. They also found that increasing the surface density of Mo on the SnO_2 increased the amount of crystalline MoO_3 and the amount of bridging Mo-O-Mo. This is from increased MoO_3 agglomeration as opposed to formation of isolated MoO_3 sites.

Figure 5: Raman of MoO_3 on Metal Oxide Supports[13]

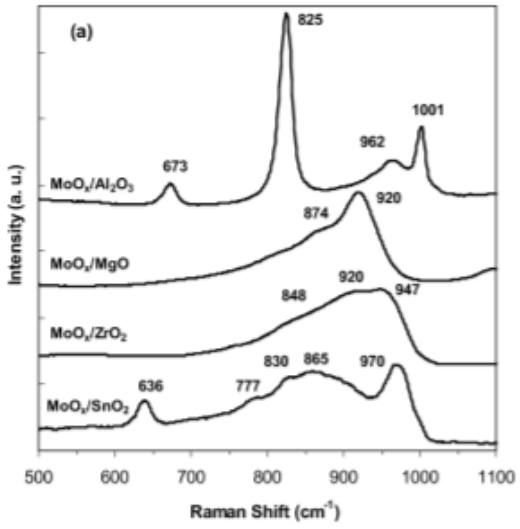

Figure 6: Raman of MoO_3 Loading on SnO_2 Support[13]

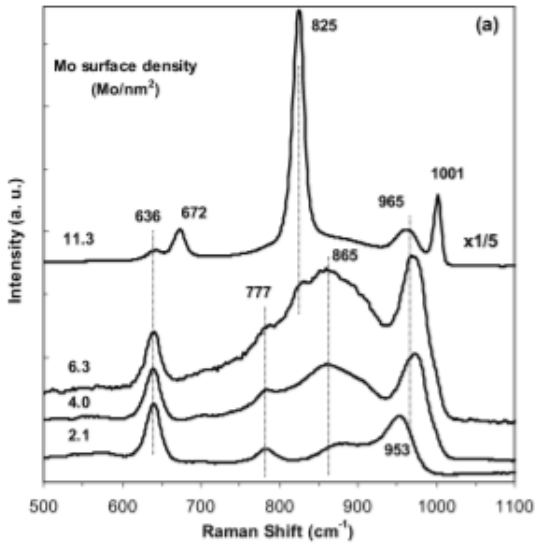

Comparing our catalyst to that of Liu, the 500 °C calcined catalyst, shown in Figure 7, matches that of the MoO_3/SnO_2 from Liu et. al. Our catalyst showed some crystallite SnO_2 peaks around 630 cm^{-1} and the terminal Mo=O between 900 cm^{-1} and 1000 cm^{-1} as seen in the Raman of the Liu catalyst. These peaks show that the 500 °C calcination yields very isolated MoO_3 domains and not large clusters of MoO_3. The 800 °C calcined catalyst, shown in Figure 8, shows more signs of large clusters. The bridging Mo-O-Mo peak at 860-870 cm^{-1} is much larger than the 500 °C catalyst and the 825 cm^{-1} associated with crystalline MoO_3 is also much larger than the 500 °C catalyst. The peaks in the 0-400 cm^{-1} region are a combination those shown in the MoO_3 control and Sn control shown in Figure 9. The larger MoO_3 clusters are probably formed from agglomeration of the individual domains as the temperature increased.

Figure 7: 500 °C Calcination Raman Spectra

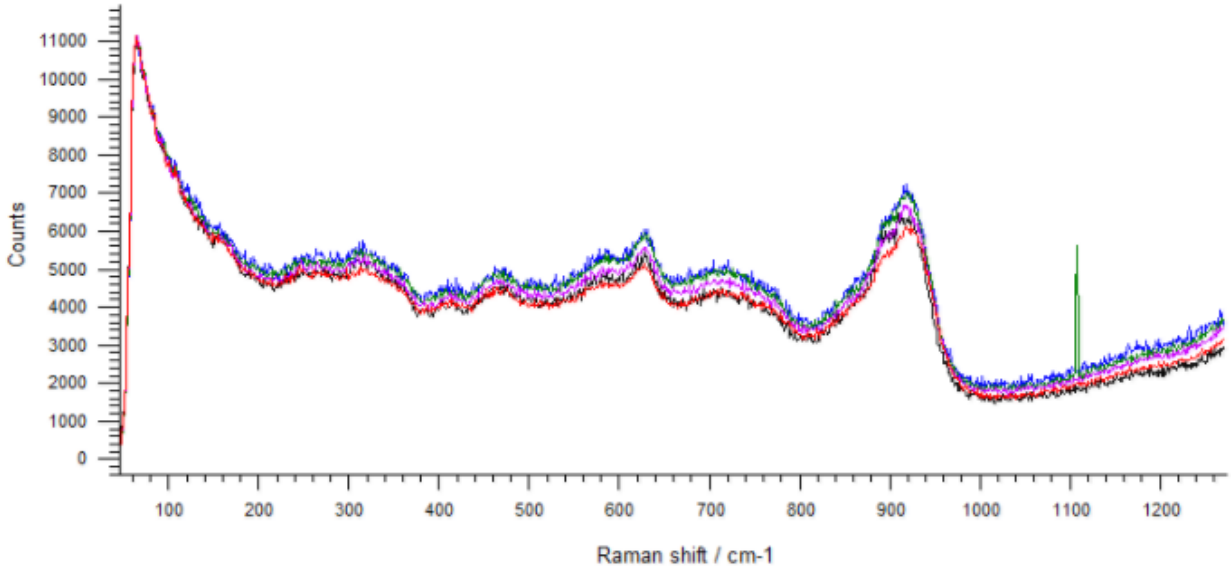

Figure 8: 800 °C Calcination Raman Spectrum

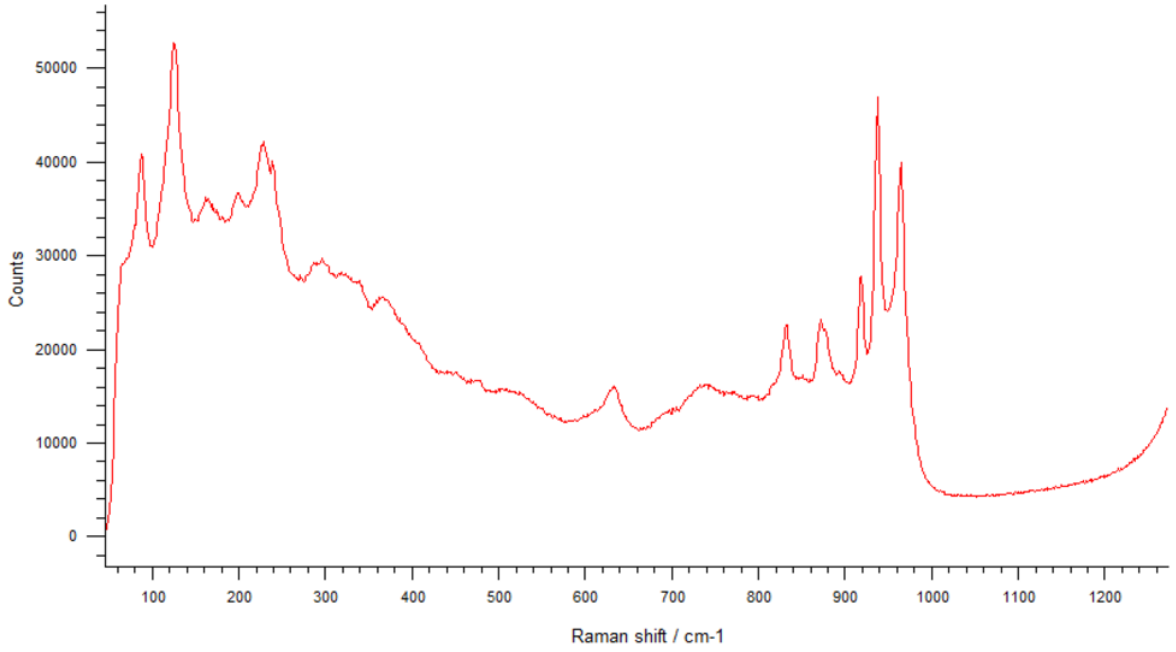

Figure 9: Comparison of Mo_3SnO_2 Catalyst to MoO_3 and SnO_2 Controls via Raman Spectroscopy

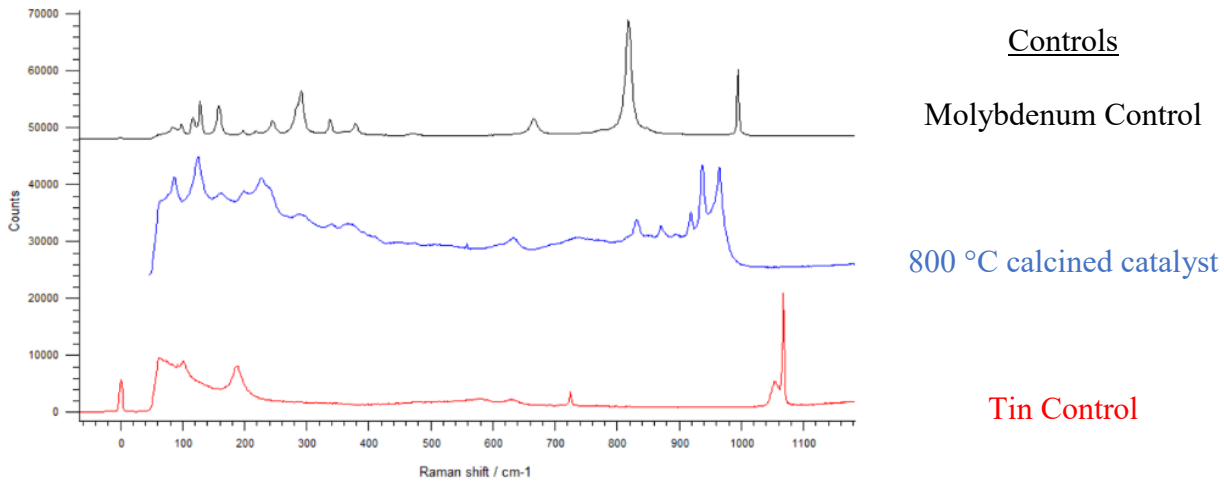

2.7 Reactions with MoO_3SnO_2

With our catalyst synthesized, we next performed a series of probing reactions to determine the reactivity of the catalyst. The reactions were mainly pulled from known reactions catalyzed by Sn-beta zeolites or Mo based catalysts. The reactions fell into several categories: aldol reactions, Baeyer-Villager reactions, ketal reactions, amide formations, and transesterifications.

2.7.1 Aldehyde Formation and Coupling

Zhang et al.'s work on dimethyl ether oxidation and coupling to form methyl formate was our starting point for MoO_3SnO_2 reactivity.[1] We hypothesized that use of diethyl ether would give comparable results to dimethyl ether, but in a liquid phase reaction as opposed to a gas phase flow system. We tested this by reacting diethyl ether in a pressure tubes under air at 50 °C

for 4 hours. As expected the reaction showed a formation of ethyl acetate. While the formation of ethyl acetate from diethyl ether is not a new or interesting reaction it served both to show that the catalyst was indeed reactive and served as a starting point for other reactions tested.

2.7.2 Aldol Reactions

Lewis acids are known to catalyze aldol reactions such as the acid catalyzed aldol reaction shown in Figure 10.[14] MoO_3SnO_2 should be able to catalyze aldol reactions as a Lewis acidic catalyst.

Figure 10: Acid Catalyzed Aldol Reaction

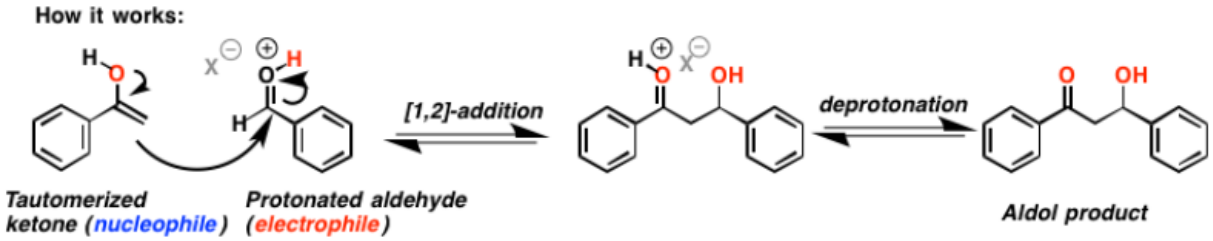

Reaction conditions from Roman-Leshkov et al. were used as a reference point in several aldol reactions.[15] A typical reaction was 0.02 mmol catalyst, 20 mmol aldehyde, 14.5 mmol ketone, stirred at 160 °C for 18 hours. MoO_3SnO_2 showed little activity as an aldol formation catalyst. In initial tests with the 500 °C catalyst there was no formation of aldol products from benzaldehyde or hexanal coupled with acetone or hydroxy acetone. When the 800 °C calcined catalyst was used in the aldol coupling reaction between benzaldehyde and acetone a small amount of aldol product, 4-Phenyl-3-buten-2-one, was formed shown in Figure 11.

Figure 11: Benzaldehyde Acetone Aldol

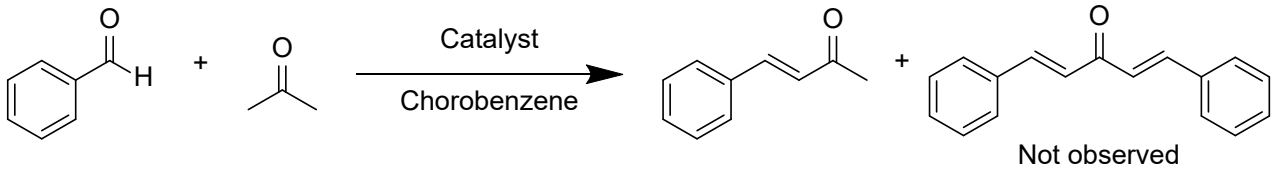

This reaction has not been fully optimized yet. However, as the single aldol product was seen and not the product from a subsequent aldol of benzaldehyde and 4-Phenyl-3-buten-2-one (dibenzalacetone), we are optimistic that it can be optimized to provide a decent and selective yield of 4-Phenyl-3-buten-2-one.

2.7.3 Baeyer-Villiger Reaction

The lactone products made in Baeyer-Villiger reactions are important in organic synthesis, as they can be used as intermediates in various fields, including pharmaceutical and agrochemical industries.[16,17] They make use of the environmentally friendly H_2O_2. SnO_2 is one of the many catalysts that has been studied and shown to be a robust catalyst in this reaction.

SnO_2 nanoparticles on a graphene oxide surface is one of these catalysts that have been shown to catalyze Baeyer-Villiger reactions with excellent conversion and selectivity (>90% and >99% respectively).[18] Molybdenum is known to form a peroxy acid when exposed to peroxides.[19] We hypothesized that our MoO_3SnO_2 catalyst would be effective in the Baeyer-Villiger reaction due to the Lewis acidic nature of the Mo peroxy acid formed from the catalyst and H_2O_2. The increased acidity of the Mo in MoO_3SnO_2 should activate the ketone in the same

manner as the SnO_2 nanoparticles and facilitate a rapid reaction from the peroxy group held near the substrate. The activation and binding of the ketone should allow for even more electronically hindered ketones to undergo Baeyer-Villiger reactions with the MoO_3SnO_2 catalyst.

In our reactions we attempted to use our catalyst to form caprolactone from cyclohexanone and hydrogen peroxide, as shown in Figure 12. Several reactions were run with 0.2 mL cyclohexanone, 0.6 mL H_2O_2 (30% w/w in H_2O), ~50 mg catalyst and 3 mL dioxane placed in a pressure vessel and heated to either 90 °C for 3 hours, 125 °C for 3 hours, or 165 °C for 18 hours. The solution was then allowed to cool to room temperature and an aliquot was analyzed by GC-MS, which showed only very small formation of the Baeyer-Villiger product. However, similar amounts of were observed when a catalyst-free control reaction was run.

Figure 12: Baeyer-Villiger Reaction

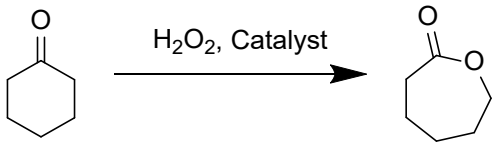

We tried other solvents because the dioxane was problematic and reacted with the peroxide or the catalyst. We tried both methanol and chlorobenzene. Methanol was also problematic, as it attacked the activated carbonyl of the cyclohexanone and caused the formation of acetal products; however, some of the products detected were probably methanol attacked Baeyer-Villiger oxidation products. This leads us to believe that the oxidation is happening, but the products are affected by the methanol. A similar non-reactive solvent should allow for Baeyer-Villiger oxidation without the unwanted reaction of methanol. The chlorobenzene didn't

cause any unwanted products; however, we were only able to detect >1% of Baeyer-Villiger oxidation products.

Nevertheless, while MoO_3 is known to form peroxy acids and be effective in many organic transformations, we believe that the combination of MoO_3SnO_2 and H_2O_2 forms too powerful of an oxidizing agent, which decomposes the organic substrates in our reactions. This reaction could be revisited with a weaker oxidant or more controlled addition of H_2O_2 to prevent the over oxidation and decomposition of the cyclohexanone.

2.7.4 Ketal Formation

Ketals are organic groups formed by the attack of alcohol groups on ketones to form a carbon center with two ether groups and two alkyl groups, as shown in Figure 13 (A and B). We sought to form a ketal from glycerol as a starting material. Ketal formation from glycerol is a known reaction and proceeds at very mild conditions.[20] However, the majority of processes give the 5-membered ring ketal as shown in Figure 13 (B); this comes from the attack of neighboring alcohol groups. Our goal was to form the less common 6-membered ring, shown in Figure 13 (A), that is a product of both terminal alcohols attacking the ketone.

Figure 13: Ketal Formation

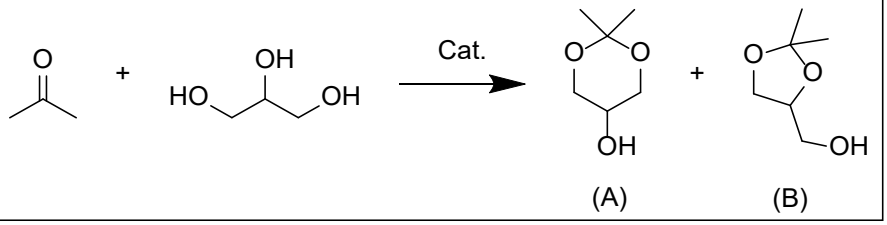

We adapted a procedure from Wegenhart et. al.[21] where 1.0 ml of acetone was mixed with 1.0 mL of glycerol and 63 mg of catalyst (calcined at both 500 and 800 °C). The reaction was stirred at 50 °C for 1 hour, then allowed to cool to room temperature. The resulting mixture was analyzed by GC-MS. While the reaction showed moderate conversion to the ketal, the 5-membered ring (B) was favored by a factor of 2:1. This shows a statistical mixture and no mechanistic selectivity for the terminal alcohols attacking over the internal alcohol. This is true for both 500 °C and 800 °C calcined catalysts.

We tried to force the formation of the 6-membered ring (A) by using an asymmetric aldehyde. Benzaldehyde was un-reactive due to the conjugation of the carbonyl into the benzyl system. Hexanal showed similar reactivity to acetone and gave comparable results of 2:1 ratio of 5- to 6-membered rings.

These experiments showed that MoO_3SnO_2 effectively catalyzed the ketal formation of acetone and glycerol. The reaction showed no selectivity toward the 6-membered ring product, which makes MoO_3SnO_2 an uninteresting catalyst in this reaction. However, a further kinetics study could give insight into the possibility of achieving selectivity with an optimized system.

2.7.5 Transesterification Reactions

Some useful organic products such as diphenyl carbonate are often formed by use of highly toxic phosgene gas.[22] To avoid the use of phosgene, transesterifications have been used in this process, such as the transformation of phenol and dimethylformate into diphenylformate and methanol. Due to the importance of this process, many catalysts are trade secrets; however, the catalysts are generally Ti based. The MoO_3SnO_2 catalyst should be a good candidate for this reaction as it has good Lewis acid sites, similar to Ti, that can activate the carbonyl and facilitate transesterification, as shown in Figure 14.

Figure 14: Dimethylcarbonate Transesterification

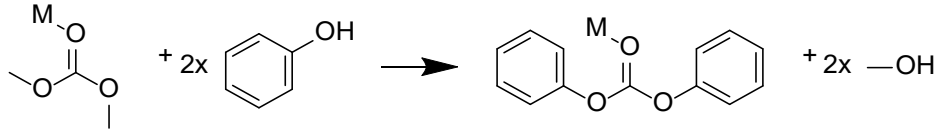

The Lewis acidity should sufficiently activate the carbonyl to facilitate attack. However, the reverse reaction is more thermodynamically favorable than the forward reaction. To make the reaction work, the methanol byproduct must be removed during the reaction process. Weiqing et al. reported on a method using a fractionary distillation column.[23]

Our lab is not equipped with a set up for circulation temperature control, so we attempted to use a similar setup with the only temperature control in the hot plate, as shown in Figure 15. A typical reaction involved addition of 3 mL phenol and 3 mL dimethyl carbonate with no solvent to a flask charged with 60 mg of catalyst. The solution was then heated to 65 °C, above the boiling point of methanol but below the boiling point of dimethylcarbonate. Repeated attempts at this procedure did not yield product. Alternatively, the same apparatus was used but the dimethylcarbonate was added slowly after the phenol was boiling. This procedure also did not yield any product. However, it is possible that a larger scale or the use of a circulating temperature control could yield better results for this catalyst.

Figure 15: Transesterification Setup

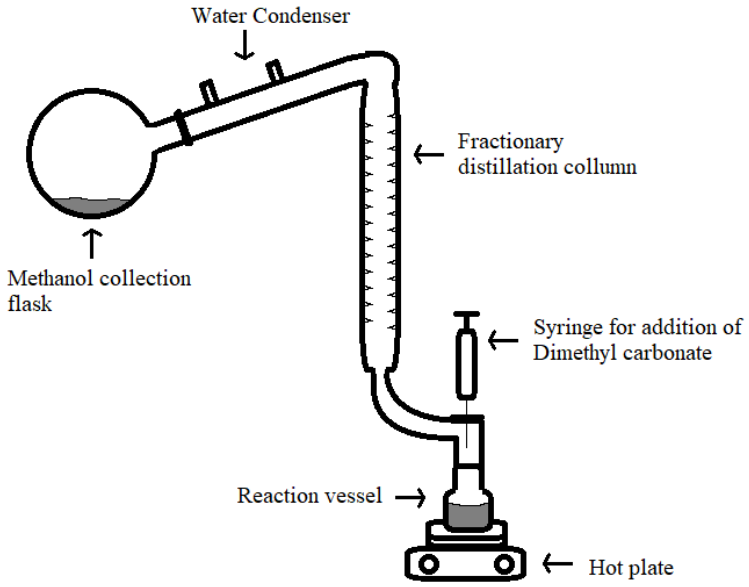

2.7.6 Formanilide Synthesis

Formanilides are small organic molecules that are congeners of formamides with an aryl group attached to the nitrogen. These molecules are used as building blocks for many pharmaceutical and industrial products.[24] The most basic formanilide, with no substitutions on the aryl ring, is simply called formanilide.

Formanilide was made from the coupling reaction of ethyl formate and aniline. The assumed mechanism is that the catalyst facilitates transformation of the ethyl formate ester into an amide, as shown in Figure 16. This is evidenced by the only visible byproduct in GC-MS being ethanol. Rasheed et al.[25] showed successful catalysis of this reaction with a sulfate catalyst immobilized on silica. This system showed excellent yield of up to 90% formanilide at 70 °C in 6 hrs. While our catalyst didn't show the same level of activity, we still were able to catalyze the

reaction to a lesser extent. We sought to use our catalyst's ability to form aldehydes and ketones from alcohols and ethers to couple the amide formation reaction to an oxidation reaction.

Figure 16: Proposed Transamidation Reaction Mechanism

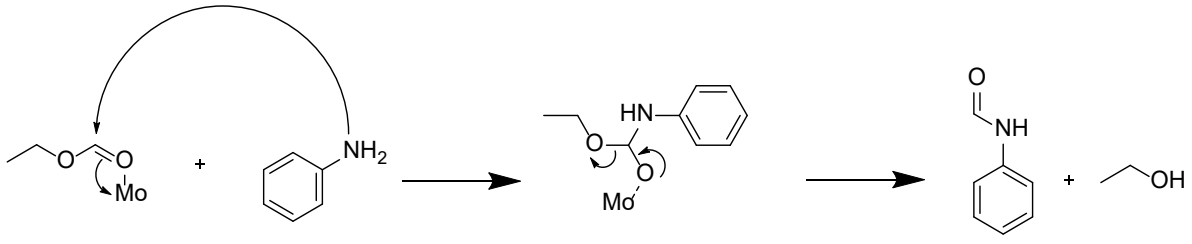

While ethyl formate is a naturally abundant source, a major goal of the Stowers' lab is the use of waste chemicals as a feedstock. Glycerol is a waste product of biodiesel production and can be oxidized to form carbon monoxide units.[26] As a precursor to using glycerol, we tested ethylene glycol as it is much easier to work with. Molybdenum peroxy acids are known to catalyze the oxidation of alcohols into ketones and aldehydes. We employed both hydrogen peroxide and molecular oxygen as the oxidant to form the molybdenum peroxy acid.

In a typical reaction, 18 µL of aniline, 21 µL of ethylene glycol, and 100 µL of 30% v/v H_2O_2 were mixed in a 7-mL vial while being heated. The vials were allowed to return to room temperature and then the products were analyzed by GC-MS.

The reaction was tested with untreated starting materials: MoO_3, SnO_2 as well uncalcined catalyst. This data is shown in Table 1. At 40 °C only materials containing Mo showed formation of products. All the molybdenum containing materials except the catalyst showed a large selectivity to nitrobenzene, formed from the oxidation of aniline. The MoO_3SnO_2 catalyst was

the only compound to show formation of the desired product formanilide. The nitrobenzene formation is probably due to the formation of the homogeneous MoO_3 peroxy acid. The MoO_3SnO_2 allows for more selective oxidation of the ethylene glycol while the increased Lewis acidity holds the newly formed carbonyl in place for attack by aniline and formation of formanilide.

Table 1: Formanilide Formation Reaction Controls

		Normalized product yields		
Control	Conversion	Nitrobenzene	Formanilide	Other Products
SnO2	0	-	-	-
MoO3	87.6	94.6	-	5.4
AHM	90.5	100	-	-
AHM (800 C cal.)	92.1	93.9	-	6.1
Sodium Stannate	0	-	-	-
Sodium S. (800 C)	0	-	-	-
Uncalcined 1:2	52.5	98.8	1.2	-
3:1 (800 C cal.)	91.2	24.9	69.8	5.3
1:2 (800 C cal.)	90.6	24.9	75.1	-

*Reaction conditions: 4 hrs, 18 µl (0.197 mmol) aniline, 21 µl (0.305 mmol) ethylene glycol, 100 µl (1.279 mmol) 30% v/v H2O2, in 2 ml chlorobenzene

Extensive experiments including time, temperature, peroxide concentration, and catalyst calcination temperature studies were all performed on the system.

Time of reaction was tested ranging from 1 hour to 16 hours as shown in Table 2. The reaction proceeds quickly, reaching 97 % completion in an hour at 50 °C. The rate of the reaction made it hard to analyze intermediates. The rate of the reaction is due to the oxidation strength of the molybdenum peroxy acid; it rapidly oxidizes the ethylene glycol.

Table 2: Time Study of Formanilide Formation Reaction

			Normalized Product Selectivity		
Entry	Time	Conversion	Aniline	Formanilide	Nitrobenzene
1	0	0.00%	100.00%	0.0%	0.0%
2	10	36.02%	96.10%	1.3%	2.6%
3	20	66.54%	89.50%	7.6%	2.8%
4	30	78.51%	75.50%	20.8%	3.7%
5	40	89.32%	56.00%	38.8%	5.2%
6	50	92.78%	34.90%	58.5%	6.6%
7	60	95.77%	25.40%	68.3%	6.3%
8	70	94.39%	22,2%	70.7%	7.1%
9	80	96.75%	17,5%	76.1%	6.4%
10	90	95.77%	19.70%	71.4%	8.9%
11	100	97.69%	16.80%	75.8%	7.4%
12	110	96.79%	17.40%	73.6%	8.9%
13	120	96.35%	16.50%	76.3%	7.2%

*Reaction conditions: 50 °C, 180 µl (0.197 mmol) aniline, 3.05 mmol alcohol, 12.79 mmol H_2O_2, in 20 ml chlorobenzene

Temperature was optimized both with and without catalyst present, the catalyst optimized reaction is shown in Table 3. With hydrogen peroxide as the oxidant, the N-formylation proceeds at moderate temperatures without the aid of a catalyst (50 °C); however, more of the side products (such as nitrobenzene) were formed based on our normalized product yields. With catalyst present, 120 °C is the optimal temperature. However, the selectivity is still not high enough for the reaction to be useful.

Table 3: Catalyzed Formanilide Reactions

Entry	Temp (°C)	Conversion	Formanilide
1	40	51.7%	11.3%
2	60	63.7%	14.5%
3	80	88.4%	22.6%
4	100	76.1%	15.8%
5	120	87.6%	29.0%

*Reaction conditions: 4 hrs, 18 µl (0.197 mmol) aniline, 21 µl (0.305 mmol) ethylene glycol, 100 µl (1.279 mmol) 30% v/v H_2O_2, in 2 ml chlorobenzene

Concentration of the peroxide was tested at 10, 30, and 50 % w/w in water. The results are shown in Table 4. The concentration of the peroxide did not have a large effect on the reaction, but 30% did give slightly better results than the other concentrations.

Table 4: Formanilide Formation Reaction Peroxide Concentration Study

			Normalized product yield		
Entry	Peroxide v/v % in Water	Conversion	Formanilide	Nitrobenzene	Other Products
1	10%	89.3%	82.8%	18.8%	0.0%
2	30%	83.0%	89.1%	10.9%	0.0%
3	50%	82.7%	81.3%	17.2%	0.0%

*Reaction conditions: 50 °C 4 hrs, 18 µl (0.197 mmol) aniline, 21 µl (0.305 mmol) ethylene glycol, 1.279 mmol H_2O_2, in 2 ml chlorobenzene

When hydrogen peroxide was used as the oxidant, some unwanted side products were formed. Azobenzene and azoxybenzene were formed by oxidation of aniline. A mass balance analysis of the data showed that not all the starting material was present in the products at the end of the reaction. When the reaction was scaled up, an analysis of many reactions showed azo- and azoxy-benzene as major products. We tested the theory that these products were sticking to the catalyst and found that azoxybenzene sticks to the catalyst. This was determined by addition of azoxybenzene, peroxide and catalyst to a solvent filled vial which was heated to 50 °C for 4 hours. The amount of azoxybenzene present decreased significantly as it stuck to the catalyst. Also, on scale up the error in mass balances of the reactions was greater than the calculated error for azoxybenzene sticking to the catalyst. The loss of mass is likely due to the strong oxidizing power of Mo with peroxide—reactants are being severely over oxidized and decomposed into small organic products that are not detected by the GC-MS.

To overcome the oxidizing power of the peroxide we experimented with using O_2 as an oxidant in a pressurized Parr reactor. The reactor was charged with 99.7 mg catalyst, 1.8 mL aniline, 2.2 mL ethylene glycol, and 6 mL methanol. The vessel was then pressurized with 8 bar of compressed air and 7 bar of N_2 to give a final pressure of 15 bar. The vessel was heated to 60 °C and stirred for 4 hours. After cooling to room temperature, the sample was worked up in methanol and tested by GC-MS. Using O_2 as an oxidant worked in the reaction, giving similar conversion, however just as with H_2O_2, unwanted azobenzene and azoxybenzene were formed by overoxidation of aniline.

2.8 Conclusions

MoO_3SnO_2 is an effective catalyst in the transformation of dimethylether to formaldehyde and methyl formate. However, to this point we have not been able to find another reaction that the catalyst can catalyze in a selective and useful manner. The formanilide reactions showed promise but could not be optimized to be selective toward a specific product.

To the best of our knowledge MoO_3SnO_2 was not able to replicate the chemistry done by Sn-based zeolites. The addition of molybdenum creates a catalyst dominated by Mo chemistry. The Mo chemistry on its own leads to unselective decomposition and over oxidation. The Sn seems to activate the Mo and facilitate even strong oxidation of substrates. But to this point the strong oxidation is non-controllable in the reactions we have tested and thus not useful until it can be controlled.

3 POLYMERIZATION OF AZIRIDINES AS A SOLID N-BASED CO_2 CAPTURE AGENT

3.1 Introduction

Increased burning of fossil fuels has caused the carbon dioxide in the atmosphere to increase significantly, with CO_2 concentration up 25.7% from fifty years ago.[27] Because of this increase, many researchers are developing new ways to handle this large concentration of atmospheric CO_2. Reduction of carbon emissions is the most widely advertised and researched solution. However, reducing CO_2 emissions doesn't immediately deal with our problem of atmospheric CO_2—we need a solution to reduce our *current* level of atmospheric CO_2. Removal of atmospheric CO_2 will lead to a decrease in the effects of current CO_2 pollution, and in the future, will aid in the creation of a carbon neutral society. Two major methods for CO_2 removal have been suggested, sequestration and storage, or upgrading. Kintisch reported on methods where CO_2 could be captured and placed in underground storage facilities.[27] Upgrading, however, is a more practical method where CO_2 is reacted with other compounds to form useful chemicals.[28] Ideally the CO_2 would be captured from the atmosphere or industrial sources prior to upgrading.

This project focused on what we feel is an important first step of CO_2 upgrading: capture of CO_2 onto a surface. Liu et al. have shown that amines are effective structures for capturing

CO_2.[29] Specifically polyethyleneimine (PEI) polymers, both branched and linear, have shown promising CO_2 capture ability. The PEI captures the CO_2 in a bifunctional mechanism that involves both electrophilic and nucleophilic parts of the PEI. First, an interaction between the nucleophilic nitrogen lone pair and the electrophilic carbon. Second, a hydrogen bond between the CO_2 oxygen and amine N-H bond.[30] Our project was an attempt to take advantage of this by grafting a branched PEI (BPEI) system onto carbon nanotubes.[31] Once good capture of CO_2 can be established, the surface can be decorated with catalyst for CO_2 upgrading reactions.

The major method that currently exists for synthesis of CO_2 capturing solid amine materials is wet impregnation of the amines onto a solid support. Wet impregnation is a physisorption technique that generally creates the non-covalent attachment of PEI to the surface of the CNTs. While physiosorbed PEI on CNT is relatively easy to prepare, it tends to have lower stability than chemisorbed compounds when exposed to higher temperatures and moisture.[32]

Wet impregnation of PEI and 3-(aminopropyl)-triethoxysilane (APTES) onto a porous silica support by Fuath et al. gave up to 37% efficiency of mol-CO_2/mol-N in a pure CO_2 stream.[33] The system also showed thermal stability up to ~350 °C at which point the PEI began to degrade. However, after several adsorption/desorption cycles the amount of amine on the surface decreased by 47%. This seems to be a significant issue with wet impregnation methods.

Another solution is preparation of these materials through chemisorption, in which amines are covalently bound to the CNT structure. This is the method that we sought to develop using small molecule building blocks as the PEI precursor. Covalent binding of PEI to the surface of CNT material should provide greater stability at high temperatures, as the material

must decompose to be removed. Also, it should provide retention of amine loading and activity through repeated use cycles.

The carbon nanotube support is made of wrapped sheets of graphene in several layers, as shown in Figure 17. This provides a large surface area for amines to be grafted onto; however, this large conjugated system makes direct attachment of amine groups difficult. Chemical functionalization of the CNT surface allows for easier attachment of amines. Nitric acid has been used to functionalize the surface CNTs with -OH and -COOH groups.[34] These functional groups can more easily react with amines to form covalently attached amine networks. Our method for attachment of PEI on CNTs is to polymerize cyclic amines using the functionalized surface as the starting point for the polymerization.

Figure 17: Multiwalled Carbon Nanotubes[35]

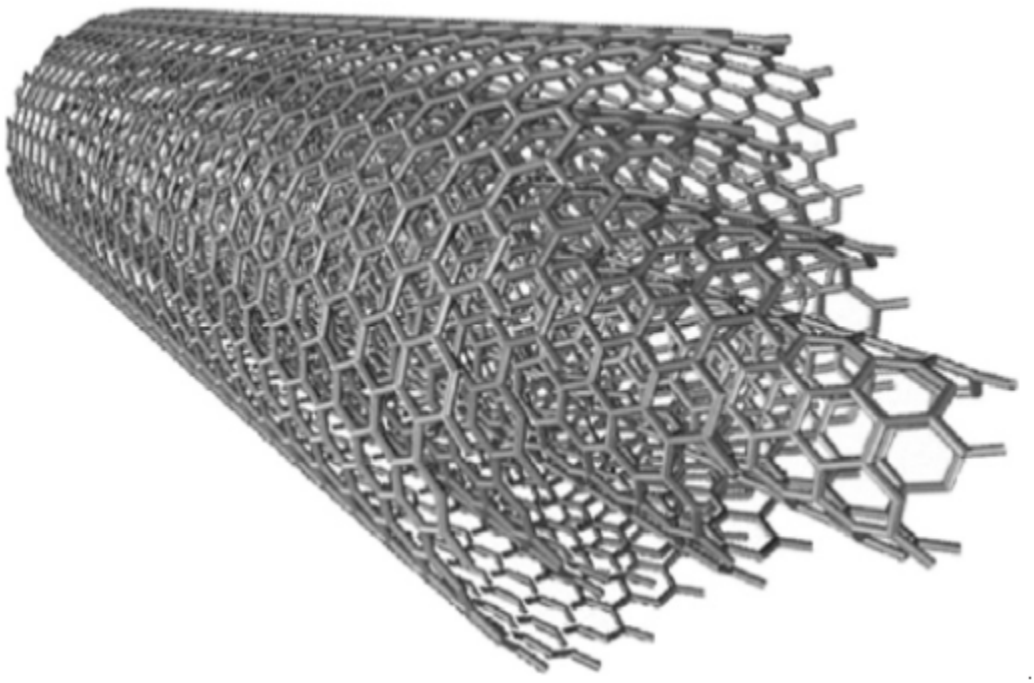

Our inspiration for polymerizing cyclic amines on to CNT came from Jones et. al.[36] Jones published a method for polymerization of aziridine onto SiO_2 surfaces by making use of the SiOH groups. Jones showed that polymerization could be achieved through ring-opening of the aziridine by hydroxy groups on the surface of a material by heating aziridine in a pressure vessel. The ring-opening of the aziridine forms a reactive species which can facilitate ring-opening polymerization to form a branched polyethyleneimine network on the surface, as shown in Figure 18. This method gave very effective loading onto the Si surface, with organic loading up to 42%.

Figure 18: Polymerization of Cyclic Amines onto SiOH Support[36]

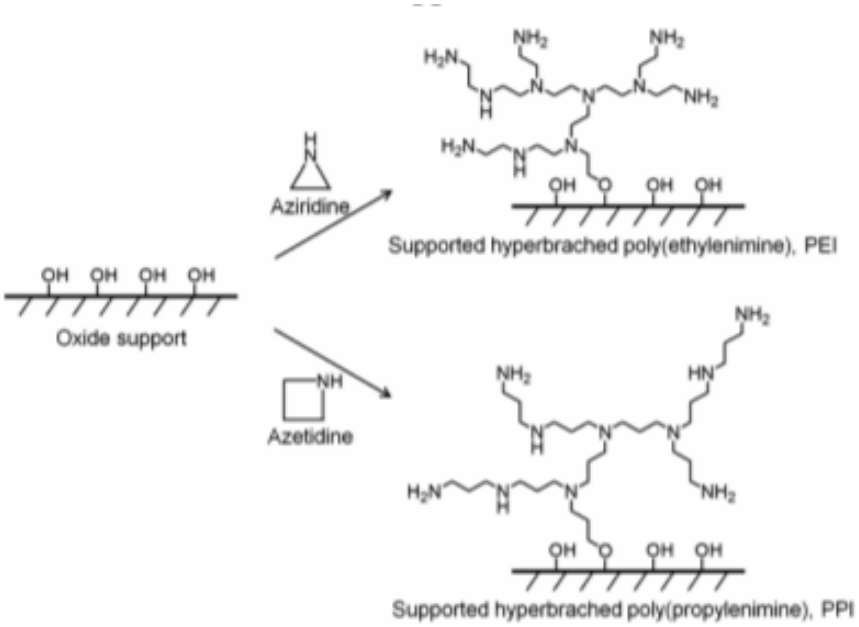

Our hypothesis was that we could apply the same technique as Jones et. al to polymerize aziridine onto the surface of carbon nanotubes for CO_2 capture, and that the covalent nature of the attachment would increase the thermal and moisture stability of the PEI. Jones found that higher acidity of the support made for more organic loading of the polymer. We hypothesized that the more acidic groups on the relatively neutral surface would still work in the polymerization. The -OH and -COOH groups on the CNT were to serve as the starting point for the polymerization. In theory the carboxylate group could cause a ring-opening of the aziridine to form the polyethyleneimine anchored by the ester group on the surface of the CNTs, as shown below in Figure 19.

Figure 19: Polymerization of Aziridine onto Functionalized CNTs

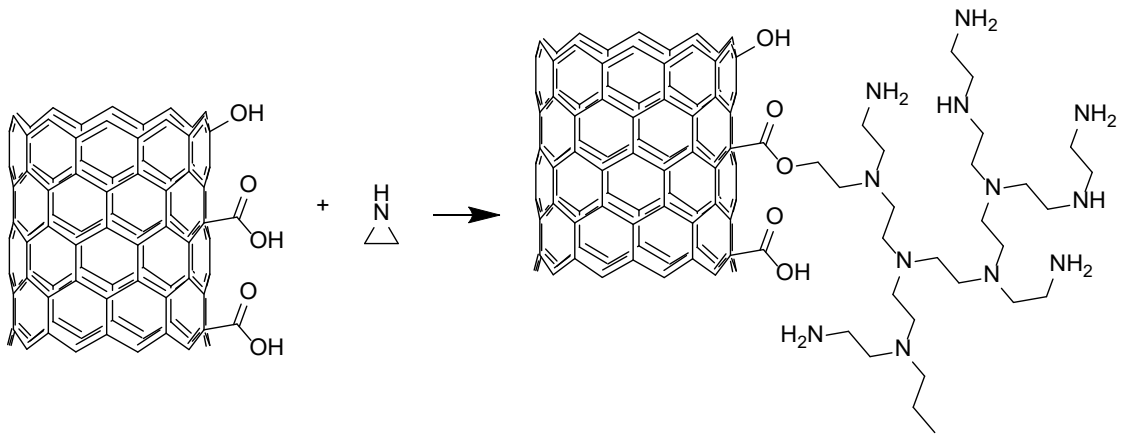

3.2 Synthesis

The general procedure for making the material consisted of several steps. First, aziridine was synthesized from 2-chloroethylamine hydrochloride. Second, CNTs were functionalized

with concentrated HNO_3. Third, the aziridine was grafted onto the CNTs (Az-CNT). After grafting, the Az-CNT was characterized through a variety of methods, including thermogravimetric analysis (TGA), FT-IR spectroscopy, Brunauer-Emmett-Teller (BET) method, and CO_2 flow reactor absorption.

3.2.1 Aziridine Synthesis

Aziridine was synthesized by a simple ring closure of 2-chloroethylamine under basic conditions as shown in Figure 20. The aziridine was extracted by partial vacuum distillation. In a typical synthesis, 8.2 g of NaOH was dissolved in 57 mL of water, then 10.2 g of 2-chloroethylamine was added. The mixture was heated to 70 °C for 2 hours, then cooled to room temperature. The flask was moved to a short path vacuum distillation apparatus and heated to 70 °C. The aziridine was distilled by slowly applying increasing vacuum to the heated system until aziridine condensed into the 0 °C trap. The distillate solution was placed in the freezer overnight to separate H_2O from aziridine. The frozen solution was warmed slightly by hand and the liquid was collected and characterized by NMR. The solution shows peaks at 0.0, wide singlet, and 1.55, singlet, corresponding to the N-H hydrogen and the C-H hydrogen. However, the aziridine wasn't successfully purified—H_2O (singlet 1.8, and singlet 4.5) was always found as a major component (>50%) in the aziridine NMR spectra.

Figure 20: Aziridine Formation

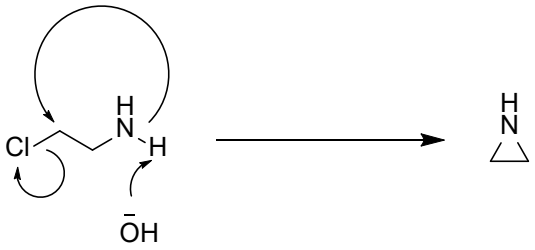

3.2.2 Carbon Nanotube Functionalization

Two types of multiwalled carbon nanotubes were used, purchased from cheaptubes.com (cheap CNT) and TCI America (TCI CNT). Both types of CNT were functionalized with carboxylic acid groups via acid treatment. In a typical synthesis, 500 mg of CNTs and enough concentrated nitric acid to completely cover them were placed in an Erlenmeyer flask fitted with a water-cooled reflux condenser. The solution was heated to reflux for 3 hours. The solution was cooled to room temperature, filtered, and rinsed with deionized water until the pH of the wash was 7, generally around 300 ml. The functionalized CNTs were then dried overnight at 90 °C.

3.2.3 Aziridine Polymerization

In a typical synthesis, 300 mg of functionalized CNTs were placed in a tall pressure tube. 1.38 g of the aqueous aziridine solution was placed in a 2-mL vial, which was placed inside of the pressure tube resting on the bed of functionalized CNTs, as shown in Figure 21. The tube was purged with N_2 for 2 minutes, then sealed and heated to 70 °C for 24 hours. The flask was

then cooled to room temperature. The pressure was released and the flask attached to a vacuum while being heated to 70 °C for 15 minutes to remove any unreacted aziridine.

Figure 21: Aziridine Polymerization Setup

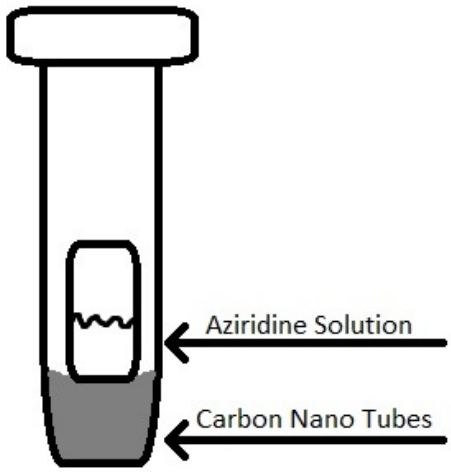

Polymerization proceeds via ring-opening of the aziridine, as shown in Figure 22. The carboxylic acid groups bound to the CNT, or the lone pair of electrons on an already attached amine, initiate the polymerization by attacking the C-N bond and starting the ring-opening. As the ring opens it can either attack another aziridine ring to continue the polymerization or attack a hydrogen to form a terminal amine.

3.2.4 Aziridine Neutralizing

Aziridine is a very hazardous chemical and so must be handled and disposed of with care. Unused aziridine was neutralized by reacting it with phenol in toluene under reflux for 4 hours. This should force the ring-opening of all aziridine by phenol to form 2-phenoxyethan-amine. The resulting mixture was disposed of as organic unwanted lab material.

3.3 Characterization

Several methods were used to characterize the final Az-CNT material. The Brunauer-Emmett-Teller (BET) method was used for surface area calculations, and the Barrett-Joyner-Halenda (BJH) adsorption method for pore volumes. Functional groups were characterized by Fourier Transform Infrared (FT-IR) spectroscopy as well as thermogravimetric analysis (TGA) for amine loading.

3.3.1 Thermogravimetric Analysis

Thermogravimetric analysis is a technique where a small sample is heated to elevated temperatures while the mass is accurately measured. Mass loss shows groups burning off the surface and can be assigned to specific groups. We used a Netzsch STA 409 PC equipped with Ar flow gas for TGA experiments.

The sample was heated from 25 °C to 600 °C at 10 °C/min under Ar flow. The mass loss from 0-100 °C is the loss of physiosorbed water on the CNTs; the large mass loss from 200-450 °C is the amine groups decomposing off the surface of the CNTs; and mass loss above 450 °C is decomposition of the CNTs. Az-CNTs were shown to have between 10 and 26% mass loading of amine groups.

Figure 23 shows the TGA data for TCI CNT, functionalized and non-functionalized, with grafted amines aziridine functionalization conditions. The functionalization of the CNTs has a significant increase on the amine loading of the grafted sample, 10% unfunctionalized vs. 26 % functionalized. This shows that more amine was grafted onto the surface when the CNTs were functionalized. The amine loading of the non-functionalized CNTs could be due to physisorption or ring-opening of aziridine by surface defects. However, the increase in amine loading does not conclusively tell if the aziridine polymerized or not.

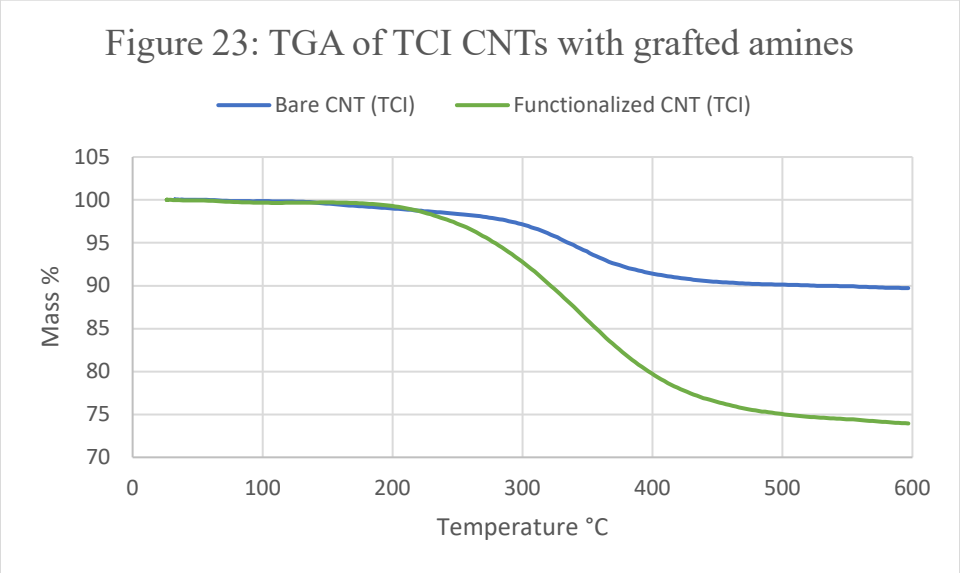

Figure 24 shows the TGA data for the cheap CNTs. There is much less of a difference between the functionalized and non-functionalized CNTs, with only about 2% more amine loading for the functionalized. The cheap CNTs are of lower quality and have not been purified as the TCI CNTs. This could mean that there are already many surface defects that can cause the ring-opening of the CNTs.

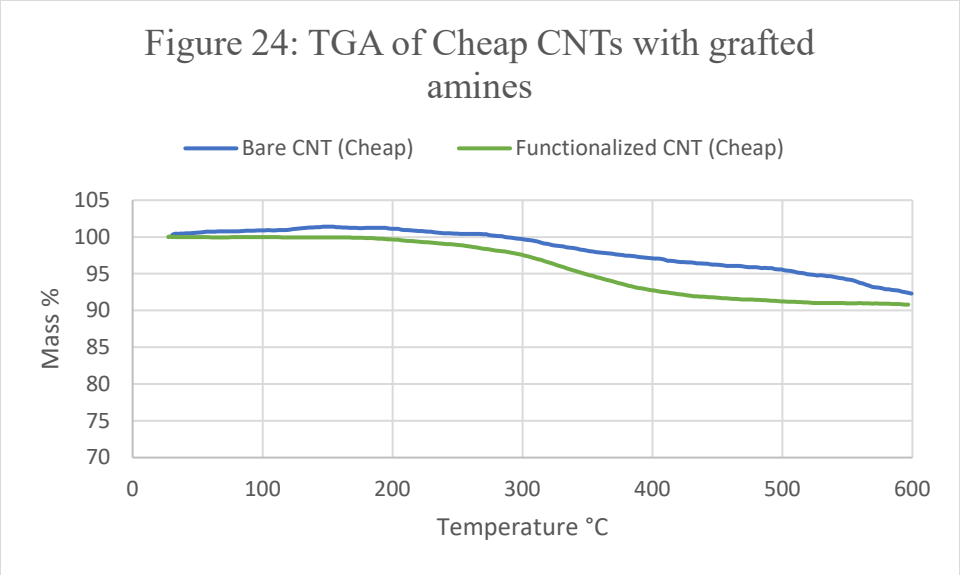

3.3.2 FT-IR Spectroscopy

A Nicolet 6700, Thermo Scientific instrument was used to measure IR absorbance from 500–2000 cm^{-1}. The very dense nature of CNTs makes spectroscopy difficult, as many of the amine functional groups reside in the pore of the CNT's structure. The dense CNTs block the IR radiation from reaching inside the pores due to the large conjugated nature of the CNTs. Only the portion of functional groups on the surface outside the pores can be measured using IR. This made it very difficult to get good, reliable data. Figure 25 shows the FTIR spectrum of pure cheap CNT. There aren't really any visible functional groups, which is probably due to the extremely conjugated nature of the CNTs. The large conjugated network absorbs most of the light and overshadows any other features, which is shown by the >50% transmittance. Figures 26 and 27 show aziridine grafted onto CNT and BPEI wet impregnated onto CNT. Neither one has any significant features (other than ambient CO_2 noise at 2360 cm^{-1}.)

Figure 25: As Is Cheaptubes CNT FTIR Spectrum

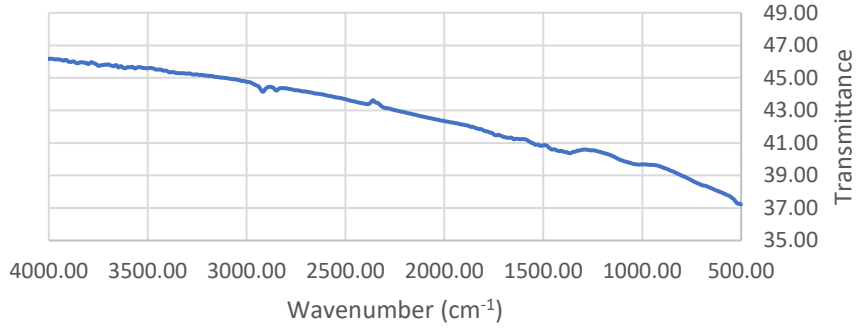

Figure 26: Az-CNT FTIR Spectrum

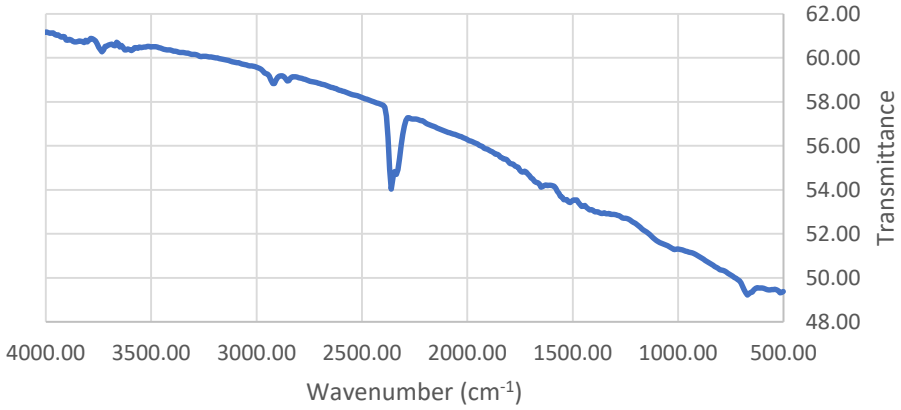

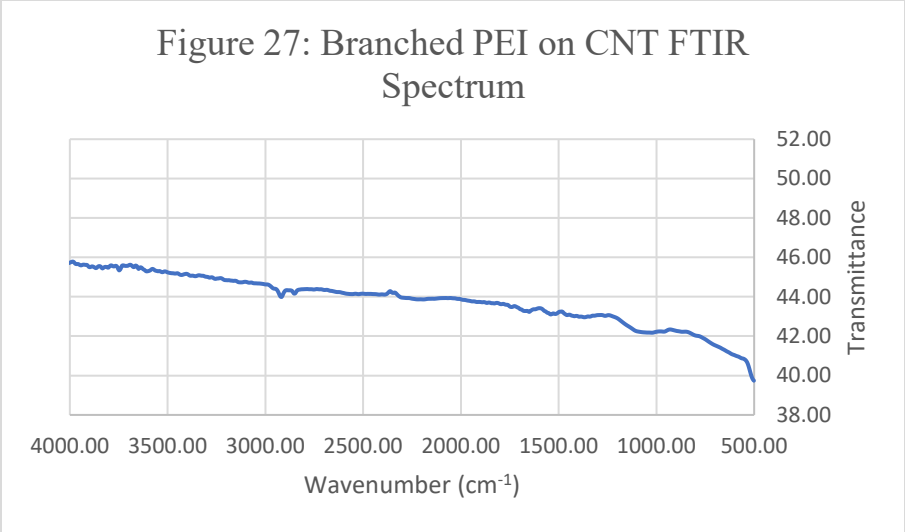

3.4 Brunauer–Emmett–Teller and Barrett-Joyner-Halenda Methods

The Brunauer-Emmett-Teller Technique (BET) method was used to determine the surface area and the Barrett-Joyner-Halenda (BJH) adsorption method to determine the pore of the material. The sample was degassed for 4 hours at 100 °C under N_2 and then run on a Micrometrics TriStar II BET instrument. BET gave the surface area of 15.4478 m^2/g and BJH gave a pore volume of 0.136513 cm^3/g. The relatively small surface area and pore volume could be due to inhibition of N_2 adsorption because of a surface covered in amine groups.

3.4.1 CO_2 Adsorption

Zheng Zhou et al. tested the materials for CO_2 adsorption.[31] The Az-CNT did not absorb as well as other tested species, 0.15 mmol CO_2/g material Az-CNT vs. 0.59 mmol CO_2/g material BPEI-CNT. With aziridine performing at ~25% of what wet impregnated BPEI did there was obviously a problem in the efficiency of the polymerization technique.

3.5 Results

Aziridine was synthesized but not successfully purified. Water was always found in the NMR spectrum of the purified aziridine. Regardless of this, aziridine was successfully grafted onto the CNT surface as evidenced by the TGA mass loss curve. Absorption data shows that Az-CNT is much less effective than BPEI-CNT at CO_2 capture; it appears that this is due to the aziridine not polymerizing and only participating in a single ring-opening reaction. So instead of polyethyleneimine groups, only a layer of primary amines was on the surface of the CNT. This could be due to the weak nucleophilic nature of the carboxyl group compared to the hydroxyl groups used by the Jones group. This could also be due to the water present in the aziridine samples as that could cause the aziridine to become protonated upon opening. This would have truncated the polymerization and only created a monomer layer.

A monomer layer of amine would prevent the chain wrapping mechanism previously described and significantly hinder CO_2 capture. This could explain the similar amine loading to BPEI but much lower CO_2 adsorption.

The method could be improved in several ways. Aziridine synthesis could be improved by increasing the scale, a larger amount of aziridine made would allow for easier distillation and purification. A purer aziridine would prevent polymerization truncation by water. Another option would be to develop a liquid phase pyridine polymerization technique, perhaps with 2-chloroethlyamine as a feedstock in presence of a non-nucleophilic base.

The surface of the CNTs were coated mostly with -COOH groups, which are less nucleophilic than -OH groups. An alternative functionalization method could be used to have a CNT surface coated with -OH vs. -COOH.

3.6 Conclusions

Aziridine ring-opening is an effective method for chemical attachment of amine groups onto functionalized carbon nanotubes. While the system has not been optimized for small scale reactions on CNT, it has been shown to graft amine groups onto the functionalized surface, as confirmed through TGA analysis. Surface areas and pore volumes were lower than expected, but this could be due to method incompatibility with polyethyleneimine. FTIR spectroscopy gave inconclusive data due to the strongly absorbing nature of CNTs.

Optimization of aziridine purification should give better polymerization and longer chains of polyethyleneimine. Longer chains should give increased CO_2 adsorption while retaining the advantages of chemisorption vs. physisorption.

4 Conclusions

In the molybdenum tin part of this work we successfully synthesized and characterized the MoO_3SnO_2 catalyst. We tested the catalyst in a wide variety of reactions with varying results. But, overall, we showed that MoO_3SnO_2 cannot act the same as Sn-beta zeolites. However, the molybdenum catalyst does display interesting reactivity that merits further investigation.

The carbon nanotube project was a greater success than the molybdenum. We were able to develop a method for grafting aziridine onto the surface on of functionalized carbon nanotubes. While polymerization did not happen, changes to the procedure could facilitate the polymerization of the aziridine.

Overall our experiments had many road blocks and showed mild success. However, we were able to successfully synthesize and characterize the amine grafted CNT and the MoO_3SnO_2 using Power X-ray diffraction crystallography, Raman spectroscopy, IR spectroscopy, GC-MS, and Thermogravimetric analysis, and both projects have potential for further research.

5 References

1. Zhang, Z.; Zhang, Q.; Jia, L.; Wang, W.; Zhang, T.; Han, Y.; Tsubaki, N.; Tan, Y. *Catal. Sci. Technol.* **2016,** *6,* 2975-2983

2. Meng, Q.; Liu, J.; Xiong, G.; Liu, X.; Liu, L.; Guo, H. *Microporous Mesoporous Mater.* **2018,** *266,* 242-251

3. Cirujano, F.G., *Catal. Sci. Technol.* **2017,** *7,* 5482-5494

4. Jin, J.; Ye, X.; Li, Y.; Wang, Y.; Li, L.; Gu, J.; Zhao, W.; Shi, J. *Dalton Trans.* **2014,** *43,* 8196

5. Hammond, C.; Conrad, S.; Hermans, I. *Angew. Chem. Int. Ed.* **2012,** *51,* 11736-11739

6. Van der Graaff, W. N. P.; Templeman, C. H. L.; Pidko, E. A.; Hensen, E. J. M. *Catal. Sci. Technol.* **2017,** *7,* 3151-3162

7. Nolan, T. B. *Chemistry of iron in natural water.* Washington, U.S. Govt. Print. Off., 1962.

8. Smedley, P. L.' Kinniburgh, D. G. *Appl. Geochem.* **2017,** *84,* 387-432

9. Kasiraju, S.; Grabow, L. C. *AlChE J.,* **2018,** advance article

10. Geng, Y.; Chen, X.; Yang, S.; Liu, F.; Shan, W. *ACS Appl. Mater. Interfaces* **2017,** *9,* 16951-16958

11. Zhang, Z.' Zhang, Q.; Jia, L.; Wang, W.; Tian, S. P.; Wang, P.; Xiao, H.; Han, Y.; Tsubaki, N.; Tan, Y. *Catal. Sci. Technol.* **2016,** *6,* 6109-6117

12. Il'in, A. A.; Dao, K. K.; Rumyantsev, R. N.; Il'in, A. P.; Petukhova, K. A.; Goryanskaya, V. A. *Russ. J. Appl. Chem.* **2017,** *90,* 1177-1182

13. Liu, H.; Cheung, P.; Iglesia, E. *J. Catal.* **2003,** *217,* 222-232

14. Mastering Organic Chemistry: The Acid Catalyzed Aldol Page https://www.masterorganicchemistry.com/2010/06/02/the-acid-catalyzed-aldol-reaction/ (accessed May 17, 2018)

15. Lewis, J. D.; Van de Vyver, S.; Roman-Leshkov, Y. *Angew. Chem. Int. Ed.* **2015,** *54,* 9835-9838

16. Hammond, C.; Conrad, S.; Hermans, I. *Angew. Chem. Int. Ed.* **2012,** *51,* 11736-11739

17. Chen, S.; Zhou, X.; Li, Y.; Luo, R.; Ji, H. *Chem. Eng. J.* **2014,** *241,* 138-144

18. Zheng, W.; Tan, R.; Luo, X.; Xing, C.; Yin, D. *Catal. Lett.* **2015,** *146,* 281-290

19. Conte, V.; Floris, B. *Dalton Trans.* **2011,** *40,* 1419

20. Ozorio, L. P.; Pianzolli, R.; Mota, M. B. S.; Mota, C. J. A. *J. Braz. Chem. Soc.* **2012,** *23,* 931-937

21. Wegenhart, B. L.; Liu, S.; Thom, M.; Stanley, D.; Abu-Omar, M. M. *ACS, Catal.* **2012,** *2,* 2524-2530

22. Niu, H.; Yao, J.; Wang, Y.; Wang, G. *J. Mol. Catal. A: Chem.* **2005,** *235,* 240-243

23. Weiqing, Z.; Xinqiang, Z.; Yanji, W.; Jiyan, Z. *Appl. Catal.* **2004,** *260,* 19-24

24. Wang, Y.; Zhan, Z.; Zhou, Y.; Lei, M.; Hu, l. *Montash. Chem.* **2018,** *149,* 527-533

25. Rasheed, Sk.; Rao, D. N.; Reddy, A. S.; Shankar, R.; Das, P. *RSC Adv.* **2015,** *5,* 10567-10574

26. Kamzolova, S. V.; Vinokurova, N. G.; Lunina, J. N.; Zelenkova, N. F.; Morgunov, I. G. *Bioresour. Technol.* **2015,** *193,* 250-255

27. Kintisch, E. *Science* **2008**, 320, 306–308

28. Wang, M.; Cao, Y.; Lie, Xi.; Wang, N.; He, L.; Li, S. *Green Chem.* **2017,** *19,* 1240-1244

29. Liu, Q.' Shi, J.; Wang, Q.; Tao, M.; He, Y.; Shi, Y. *Ind. Eng. Chem. Res.* **2014**, *53*, 17468–17475.

30. Thirion, D.; Rozyyev, V.; Park, P.; Byun, J.; Atilhan, M.; Yavuz, C. T. *Phys. Chem. Chem. Phys.* **2016,** *18,* 14177-14181

31. Zhou, Z.; Anderson, C. M.; Butler, S. K.; Thompson, S. K.; Whitty, K. J.; Shen, T.-C.; Stowers, K. J. *J. Mater. Chem. A.* **2017,** *5,* 10486-10494

32. Liu, Y.; Ye, Q.; Shen, M.; Shi, J.; Chen, J.; an, H.; Shi, Y. *Environ. Sci. Technol.* **2011,** 45, 5710–5716.

33. Fauth, D. J.; Gray, M. L.; Pennline, H. W.; Krutka, H. M.; Sjostrom, S.; Ault, A. M. *Energy Fuels* **2012,** 26, 2483–2496.

34. S. Mathur, S. S. Ray, S. Widjaja and D. Singh, *Nanostructured Materials and Nanotechnology V: Ceramic Engineering and Science Proceedings*, **2011,** *32,* 43–51.

35. Zannotti, M.; Giovannetti, R.; D'Amato, C. A.; Rommozzi, E. *Spectrochim. Acta, Part A* **2016,** *153,* 22-29

36. Chaikittisilp, W.; Didas, S. A.; Kim, H.; Jones, C. W. *Chem. Mater.* **2013,** *25,* 613-622